Circulating extracellular vesicles as non-invasive biomarker of rejection in heart transplant

(Article begins on next page)

18 September 2024

Circulating Extracellular Vesicles as a Noninvasive Biomarker of Rejection in Heart Transplant

C. Castellani[1*], J. Burrello[2*], M. Fedrigo[1], A. Burrello,[3] S. Bolis[2],

D. Di Silvestre[4], F. Tona[5], T. Bottio[5], V.Biemmi[2,7], G. Toscano[5], G. Gerosa[5], G. Thiene[1],

C. Basso[1], S.L. Longnus[6], G. Vassalli[2,7], A. Angelini[1#], L. Barile[2,7,8#].

(1) Cardiovascular Pathology and Pathological Anatomy, Department of Cardiac, Thoracic, Vascular Sciences and Public Health, University of Padova, Padova, Italy. (2) Laboratory of Cellular and Molecular Cardiology and Laboratory for Cardiovascular Theranostics, Cardiocentro Ticino Foundation, Lugano, Switzerland. (3) Department of Electrical, Electronic and Information Engineering "Guglielmo Marconi" (DEI), University of Bologna, Italy. (4) Proteomics and Metabolomic Lab, ITB-CNR, Segrate, Italy. (5) Division of Cardiac Surgery, Dept. of Cardiac-Thoracic Vascular Sciences and Public Health, University of Padua, Italy. (6) Department of Cardiovascular Surgery, Inselspital, Bern University Hospital, Bern, Switzerland. (7) Faculty of Biomedical Sciences, Università Svizzera Italiana, Lugano, Switzerland. (8) Institute of Life Science, Scuola Superiore Sant'Anna, Pisa, Italy.

[*]Equally contributing first authors. #Equally contributing last authors.

Manuscript word count: 6990 including references and figure captions. Abstract word count: 250

Number of Tables: 1; Number of Figures: 6.

Supplementary data: 11 Supplementary Tables and 2 Supplementary Figures.

Addresses for correspondence:

Annalisa Angelini (email: annalisa.angelini@unipd.it) – Department of Cardiac, Thoracic, Vascular Sciences and Public Health, University of Padova - Via A. Gabelli 61, 35121 – Padova (Italy)

Lucio Barile (email: lucio.barile@cardiocentro.org) – Laboratory for Cardiovascular Theranostics, Cardiocentro Ticino Foundation - Via Tesserete 48, 6900 – Lugano (Switzerland).

1 **ABSTRACT**

2 *Aims* – Circulating extracellular vesicles (EV) are raising considerable interest as a non-invasive

3 diagnostic tool as they are easily detectable in biological fluids and contain specific set of nucleic acids,

4 proteins, and lipids reflecting pathophysiological conditions. We aimed to investigate differences in

5 plasma-derived EV surface-protein profile as biomarker to be used in combination with endomyocardial

6 biopsies (EMB) for the diagnosis of allograft rejection.

7 *Methods and results* – Plasma was collected from 90 patients (53 training cohort, 37 validation cohort)

8 prior to EMB. EV concentration was assessed by nanoparticle tracking analysis. EV surface antigens

9 were measured using a multiplex flow cytometry assay comprising 37 fluorescently labelled capture bead

10 populations coated with specific antibodies directed against respective EV surface epitopes. The

11 concentration of EV was significantly increased and their diameter decreased in patients undergoing

12 rejection as compared to negative ones. The trend was highly significant for both antibody-mediated

13 rejection (AMR), and acute cellular rejection ($P<0.001$). Among EV-surface markers, CD3, CD2, ROR1,

14 SSEA-4, HLA-I, and CD41b were identified as discriminants between controls and ACR, whereas HLA-

15 II, CD326, CD19, CD25, CD20, ROR1, SSEA-4, HLA-I, and CD41b discriminated controls from

16 patients with AMR. ROC curves confirmed a reliable diagnostic performance for each single marker

17 (AUC range 0.727-0.939). According to differential EV-marker expression, a diagnostic model was built

18 and validated in an external cohort of patients. Our model was able to distinguish patients undergoing

19 rejection from those without rejection. The accuracy at validation in an independent external cohort

20 reached 86.5%. Its application for patient management has the potential to reduce the number of EMBs.

21 Further studies in a higher number of patients are required to validate this approach for clinical purpose.

22 *Conclusions* - Circulating EV are highly promising as new tool to characterize cardiac allograft rejection

23 and to be complementary to EMB monitoring.

NARRATIVE ABSTRACT - Our study describes a method for detecting and characterising circulating extracellular vesicles (EV) as a minimally invasive, liquid biopsy for the diagnosis of cardiac allograft rejection, and as a complementary tool to EMB monitoring. EV obtained from peripheral blood were profiled to identify rejection and its types in cardiac transplant recipients. A standardized and rapid tool was established using a fluorescent bead-based multiplex assay. We built a diagnostic model based on machine learning algorithms to identify non-rejecting patients who potentially do not require EMBs. EV profiling could represent a tool for non-invasive monitoring of allograft rejection in cardiac transplant recipients.

Keywords: Extracellular Vesicles; Allograft Rejection; Heart Transplant; Biomarker; Machine Learning.

ABBREVIATION LIST: EMB, endomyocardial biopsy; ACR, acute cellular rejection; AMR, antibody-mediated rejection; EV, extracellular vesicles; NTA, nanoparticle tracking analysis; FC, flow cytometry; MFI, median fluorescence intensity; RF, random forest; DSA, donor-specific antibody.

INTRODUCTION

Allograft rejection remains a serious complication during and after the first post-transplant year[1, 2]. More than 25% of patients have rejection episodes within one year and face the risk of developing consequent graft dysfunction with increased morbidity and mortality[3]. Thus, early detection of cardiac allograft rejection is crucial to lower the risk of late morbidity and mortality. The current gold standard for diagnosis and grading of rejection is via endomyocardial biopsy (EMB). EMB is performed either to confirm clinical diagnosis of allograft rejection, or routinely in asymptomatic patients, as surveillance

2

48   monitoring for rejection(4, 5). EMB has also been used to evaluate efficacy of immunosuppression

49   therapies in several clinical trials in which patients underwent more than 10 EMB during the first year

50   after transplant(6, 7). This procedure still faces unresolved issues such as invasive risk, sampling error,

51   and inter-reader variability(8-10). There is a long-standing effort toward the discovery of sensitive and

52   noninvasive methods for the diagnosis of rejection that could be used in combination with tissue

53   histology for reducing the frequency of biopsies(11). New, promising approaches are based on genomic

54   screening, including microRNA(12, 13), and mRNA profiling(14). The non-invasive detection of

55   circulating cell-free DNA (cfDNA)(15), or graft-derived cell-free DNA (GcfDNA)(16) were also

56   proposed to diagnose acute cellular rejection (ACR), but not antibody-mediated rejection (AMR).

57   Because nucleic acids and cell-free proteins are unstable in the circulation, a reliable quantification

58   remains a critical problem.

59   Cells secrete extracellular vesicles (EV) that are composed of bioactive molecules mediating intercellular

60   communication processes(17) and activating intracellular signalling pathways of target cells(18, 19). EV

61   released into the circulation and body fluids display different RNA, protein, and lipid contents reflecting

62   the homeostatic state and function of EV-producing cells. A change in the pathophysiological status of

63   tissues and/or organs affects the composition of circulating EV, resulting in a specific molecular

64   signature(20-22). This is of particular interest with regard to acute inflammatory processes, since EV

65   have emerged as key regulators in immune responses(23-25). In this context, EV have great potential as

66   diagnostic biomarkers in various diseases, including cardiovascular diseases(22) and might represent a

67   valuable tool to support EMB in the diagnosis of different types of cardiac rejection. Given its limited

68   invasiveness, the profiling of blood-derived EV represents an interesting diagnostic approach for

69   monitoring early, post-transplant status and for therapeutic management of patients.

70   Here, we assessed, in a clinical setting, the potential of surface profiling of circulating EV for the

71   diagnosis of acute cardiac allograft rejection, as companion biomarker to EMB monitoring. A multiplex

72 flow cytometric assay using antibody-coated capture beads was used to investigate differences in EV

73 antigen expression in patients with an EMB diagnosis of ACR or AMR. Differentially expressed EV-

74 surface antigens were combined in a single diagnostic model, based on machine learning algorithms,

75 allowing for high accuracy discrimination between patients with and without graft rejection and among

76 the different types of rejection. Finally, we validated our computational approach in an independent

77 cohort of patients.

78

79 **METHODS**

80 A detailed description of patient data, EV isolation and characterization protocols, statistical analyses,

81 and diagnostic modelling is provided in the Supplementary Appendix.

82 *Patient selection and blood handling*

83 Patients undergoing heart transplant were recruited at the Cardio-Surgery Center Gallucci (Dept. of

84 Cardiac-Thoracic-Vascular Sciences and Public Health at the University Hospital of Padua, Italy). The

85 study was approved by the local ethical committee and fully informed, written consent was provided by

86 each patient. A total of 90 plasma samples were included and split into a training set (n=53) and a

87 validation cohort (n=37). Patients with a first episode of rejection within 1 year since transplant were

88 included in the study. Patients without rejection episodes within 1 year since transplant were enrolled as

89 controls (Rejection 0, R0).

90 Patients from the training cohort were retrospectively selected between February 2018 and March 2019,

91 including only subjects with an unequivocal diagnosis at EMB. According to the ISHLT classification

92 for ACR, we selected EMBs showing 2R or 3A grade that correspond to multifocal inflammatory

93 infiltrate, and multiple foci of myocyte necrosis. For AMR diagnosis, we selected EMBs corresponding

94 to pAMR 1(I+) or pAMR 2, in presence of positivity for circulating donor specific antibodies.

95 For the validation cohort, we included 37 unselected consecutive patients, admitted for EBM between

96   April 2019 and January 2020, regardless of the final histologic diagnosis.

97   We excluded, from both validation and training cohorts, patients with other acute or chronic

98   inflammatory disease (e.g., auto-immune disease, cancer, active infections).

99   All transplanted patients were ABO-compatible and were treated with cyclosporine, mycophenolate, and

100   corticosteroids. All subjects enrolled in our study were scheduled for a surveillance biopsy in their regular

101   follow-up after heart transplant in a setting of stable allograft function. Patients did not display any

102   clinical signs/symptoms related to graft rejection (none of the patients was enrolled because rejection

103   was suspected). Blood sampling was performed immediately before the EMB, thus avoiding potential

104   confounding factors associated to procedure-related injury.

105   The diagnosis of either ACR or AMR was defined, according to the International Society for Heart and

106   Lung Transplantation guidelines (4, 5) (see Supplementary Appendix).

107   Blood was collected in EDTA-treated tubes and centrifuged at 1,600 g for 15 minutes to separate plasma

108   from cellular components; the low centrifuge speed avoided shear-stress-induced platelet activation.

109   Plasma underwent serial centrifugation cycles to remove intact cells, cellular debris and larger EV:

110   3,000 g for 20 minutes, 10,000 g for 15 minutes, and 20,000 g for 30 minutes (Figure 1A). Cleared,

111   platelet-free plasma was finally stored at -80°C and not thawed prior to analysis.

112   *Plasma-derived EV quantification*

113   Presence of specific EV markers and absence of apolipoprotein contaminants were assessed by western

114   blotting. Size and concentration of plasma EV were determined by nanoparticle tracking analysis (NTA)

115   using NanoSight LM10 (*Malvern Instruments, UK*) equipped with a 405 nm laser and Nanoparticle

116   Tracking Analysis NTA 2.3 analytic software. EV concentration is shown as EV/mL (median value,

117   interquartile range).

118   *EV surface marker analysis by multiplex flow cytometry*

119   All samples underwent bead-based EV immunocapture and were analyzed by flow cytometry (FC),

120   using MACSPlex human Exosome Kit (*Miltenyi Biotec, Germany*), according to manufacturer's

121   instructions. Median fluorescence intensity (MFI) was measured on a MACSQuant Analyzer 10 flow

122   cytometer according to previous validation studies(26-29). The multiplex platform analysis and

123   gating strategy have previously been described(26, 28). MFI was evaluated for each subset of capture

124   beads, corrected by subtracting the MFI of corresponding blank controls, and normalized by the mean

125   MFI of CD9, CD63, and CD81.

126   *Statistical analysis and diagnostic modelling*

127   IBM SPSS Statistics 22 (IBM Corp., Armonk, New York, USA) and GraphPad PRISM 7.0a (La Jolla,

128   California, USA) were used for statistical analyses. Scalar variables were analyzed with Kolmogorov–

129   Smirnov test to evaluate distributions. Normally distributed variables are expressed as mean ± standard

130   deviation and were analyzed by ANOVA with post-hoc Bonferroni's tests; non-normally distributed

131   variables are expressed as median [interquartile range] and were analyzed by Kruskal-Wallis tests.

132   Categorical variables are expressed as absolute number (percentage) and were compared with chi-square

133   tests (Fisher's exact test when sample size was ≤ 5). Correlations were evaluated by Pearson's test (R

134   coefficient) and analysis of regression curves. Receiver operating characteristics (ROC) curves were used

135   to assess the area under the curve (AUC) and to compare diagnostic performances of selected variables;

136   the Younden Index (J = sensitivity + specificity - 1) was calculated to assess the best sensitivity and

137   specificity. *P*-values of less than 0.05 were considered significant.

138   Machine learning supervised algorithms are exploited in clinical practice to formulate predictions of

139   selected outcomes based on a given set of labeled, paired, input-output training sample data(30, 31). To

140   build the diagnostic model, a random forest (RF) algorithm was created using Python 3.5 (library, scikit-

141   learn). The algorithm created 40 different classification trees; if at least 21 of 40 trees of the RF indicate

142   the absence of rejection, the patient was classified as R0 (level 1); in case of detection of graft rejection,

143   a second RF algorithm was created to distinguish ACR from AMR (level 2). A combined model was also

144 built to distinguish R0 *vs.* ACR *vs.* AMR, in a single step. Models were both internally and externally

145 validated. Internal validation was provided by a leave-one-out cross-validation algorithm (see

146 Supplementary Appendix). External validation was performed on an independent cohort enrolled in the

147 same center.

148 *Protein interactor network analysis*

149 Protein interactors of the EV-surface marker were retrieved by Cytoscape PESCA plugin(32) and a

150 global *Homo sapiens* protein-protein interaction (PPI) network of 1588 nodes and 36984 edges was

151 reconstructed. For each quantitative comparison (R0 *vs.* ACR and R0 *vs.* AMR), a specific PPI sub-

152 network per comparison was reconstructed considering the first neighbors of each differentially

153 expressed EV-surface marker protein.

154

155 **RESULTS**

156 *Patient characteristics*

157 We enrolled 90 subjects, 53 in the training cohort and 37 in the validation cohort. Patient characteristics

158 are summarized in Tables 1, S1, and S2. All subjects enrolled were scheduled for a surveillance biopsy

159 in their regular follow-up in a setting of stable allograft function.

160 According to EMB parameters and biochemical analyses, patients from training cohort were divided in

161 three groups (R0, ACR, AMR). They were similar with respect to sex and age, whereas the time from

162 heart transplant to rejection was 3 [2;8] months for the ACR group compared to 11 [9;14] months for the

163 AMR group (*P*=0.004). Among AMR patients, 4 of 9 (44.4%) presented with capillary deposition of

164 complement fraction C4d, and 2 of 9 (22.2%), with CD68-positive staining in macrophages with a

165 grading >10%. The anti-HLA antibody assessment revealed all AMR patients as positive for anti-HLA-

166 II donor-specific antibodies (DSA) and anti-HLAII non-DSA. Moreover, 8 of 9 (88.9%) patients in the

167 AMR group displayed a strong positivity for anti-HLA-I non-DSA. As expected, the cellular rejection

168   score was higher in patients with ACR compared to both controls and AMR patients. Biochemical

169   parameters and the ejection fraction at echocardiography are reported in Table S2. For diagnostic

170   modelling purpose, an independent cohort was enrolled. Clinical, biochemical, and EMB parameters did

171   not significantly differ from the training cohort (Table S3).

172   *EV quantification*

173   The immunocapture assay was validated for its specificity to bind vesicles by western blotting analysis

174   for the presence of specific EV markers such as TSG101 and CD81 and for the absence of contaminants

175   such as apolipoprotein (ApoB48; Figure 1B). Given the reliability of the immunocapture protocol, we

176   used the level of expression of tetraspanins CD9, CD63, and CD81 (generally accepted EV surface

177   markers) for specific quantification of circulating EV. The MFI of tetraspanins was higher in patients

178   with ACR and AMR, compared to R0 ($P<0.001$; Figure 1C and Table S4).

179   Size and concentration profiles of circulating EV were determined by NTA. NTA confirmed a significant

180   increase of the concentration of plasma-derived EV in patients undergoing rejection compared to subjects

181   classified as R0; no differences were observed between ACR and AMR (Figure S1A and Table S4).

182   Overall, the increase in the total number of EV reflects a concentration of the smaller subset (30-150 nm)

183   that was approximately three-fold higher in ACR and AMR compared to R0 ($P<0.01$ for both

184   comparisons; Figure S1A). Consistently, the median EV diameter was significantly lower in ACR and

185   AMR *vs.* R0 ($P<0.001$; Figure S1B and Table S4). Cumulative distribution plots (EV concentration *vs.*

186   particle size), resulted in a left-shift of curves and higher AUC for ACR and AMR as compared to R0

187   ($P<0.001$ for both; Figure 1D). Although NTA cannot distinguish EV from other particles such as

188   lipoproteins, the analysis correlates with the antigenic quantification of CD9/CD63/CD81 (Pearson's

189   R=0.463; $P<0.001$; Figure 1E).

190   *Analysis of EV-surface markers*

191 Immunocaptured EV from pre-cleared plasma of patients from the training cohort (n=53) were analyzed

192 for the expression of 37 different surface antigens (Table S5). Several biomarkers were significantly

193 higher in both ACR and AMR patients compared to R0 (Figure 2A). This applied for four antigens

194 including the molecules of major histocompatibility complex class-I (HLA-I), the platelet membrane

195 glycoprotein II-b (CD41b) and two non-immune system-related antigens: tyrosine-protein kinase

196 transmembrane receptor (ROR1) and Stage-Specific Embryonic Antigen-4 (SSEA-4). Expression levels

197 of two T-cell surface antigens, CD2 and CD3, that function as a cell adhesion molecule and a co-receptor

198 activator, respectively, were differentially expressed between ACR patients *vs.* R0. In addition, the

199 surface EV expression of five, well-established, immunologic markers was significantly higher in AMR

200 patients as compared to R0: major histocompatibility complex class II (HLA-II), the epithelial cell

201 adhesion molecule (CD326), B-lymphocyte antigens CD19 and CD20 and the interleukin-2 receptor

202 alpha chain (CD25). Compared to R0, the heatmap highlights clusters corresponding to high MFI for

203 CD2, CD3, ROR1, SSEA-4, HLA-I and CD41b in ACR patients, and to high ROR1, SSEA-4, HLA-I,

204 CD41b, HLA-II, CD326, CD19, CD25, and CD20 in AMR patients (Figure 2B).

205 *Diagnostic Modelling*

206 The power of discrimination between patients presenting graft rejection and non-rejecting R0 controls

207 was evaluated by analysis of ROC curves for each single, differentially expressed EV-surface marker.

208 Overall, the MFI analysis displayed a reliable diagnostic performance for all the evaluated markers

209 (Figure 3). Comparing ACR *vs.* R0, the best performance was obtained for HLA-I (AUC 0.939), CD3

210 (AUC 0.848) and SSEA-4 (AUC 0.832), CD2 (AUC 0.829). Of note, the MFI for EV-carried HLA-I,

211 CD2 and SSEA-4 displayed a sensitivity of 100% in the diagnosis of ACR, with specificities ranging

212 between 63.6 and 87.9% (Figure 3A, and 3C). For AMR *vs.* R0, ROR1 showed the best performance

213 with an AUC of 0.879 (sensitivity and specificity of 100% and 75.8%, respectively), followed by HLA-

214 I (AUC 0.872), SSEA-4 (AUC 0.820), CD20 (AUC 0.798), CD19 (AUC 0.795), HLA-II (AUC 0.788),

215 and CD41b (AUC 0.778). Strengthening our results, ROR1, SSEA-4, HLA-II and CD41b each achieved

216 100% sensitivity, correctly identifying all patients with AMR (Figure 3B, and 3D).

217 After having demonstrated excellent diagnostic performances for each candidate biomarker considered

218 individually, we combined the 11 differentially expressed EV-surface antigens in a single diagnostic

219 model using machine learning algorithms. A RF classification model was used as computational

220 approach to identify patients with heart rejection using the MFI of circulating EV-carried antigens

221 (Figure 4). The RF model was developed in the training cohort (n=53) and then internally validated by a

222 leave-one-out cross-validation algorithm (see methods), which simulated how the model could generalize

223 on an independent cohort. Finally, we performed a real external validation of the RF model on an

224 independent cohort enrolled in the same center.

225 At the training, a double level RF model was built as a first approach: the first level discriminated the

226 presence of rejection (including both ACR and AMR) *vs.* no-rejection (R0) with an accuracy of 100%.

227 All identified rejecting subjects (n=20), were then introduced in the second level, to distinguish between

228 the two rejection types (ACR *vs.* AMR); this second model also provided a very high performance with

229 an accuracy of 95%. All patients except one were correctly identified; a single patient with AMR was

230 classified as ACR (Figure 4A). Next, we built a combined model to classify patients in one single step

231 (R0 *vs.* ACR *vs.* AMR); all subjects were correctly allocated with an accuracy of 100% (Figure 4B). We

232 then provided an internal validation by a leave-one-out cross-validation algorithm to simulate how the

233 algorithms could perform in an independent cohort and to exclude overfitting bias (effect due to the best

234 performance of the model in the cohort in which it is trained). The accuracy was still very high (83% to

235 88.7%), with a modest overfitting effect (11.3% to 17%). Finally, we tested our model in an independent

236 external validation cohort (Figure 5). Consistently with the internal validation, the accuracy was 86.5%,

237 81.3%, and 78.4%, respectively for level 1, level 2, and combined RF models, thus confirming a reliable

238 diagnostic performance even in an external cohort of patients.

239 The enrollment of consecutive unselected patients in the validation cohort, allowed us to simulate a

240 clinical context in which EV profiling and random forest model were integrated not to avoid EMBs, but

241 to select patients for this procedure. With this approach, we would have correctly managed 34 of 37

242 patients (accuracy 91.9%), while reducing by 56.8% the number of EMBs required (Figure 6).

243 Unfortunately, 3 rejecting patients would have been predicted as R0, thus missing the possibility to be

244 correctly managed by EMBs.

245 *Correlation analyses*

246 Patients from training and validation cohorts were pooled and correlation analyses were performed to

247 evaluate whether expression levels of EV-surface markers and EV concentration might relate to EMB

248 findings and/or patient characteristics. Cellular rejection score correlates with EV concentration and with

249 the expression level of SSEA-4, HLA-I, CD41b (R range 0.323-0.581, $P<0.01$) in patients with ACR.

250 Significant correlations have been also found between circulating levels of anti-HLA-I (DSA and non-

251 DSA), and anti-HLA-II (DSA and non-DSA) antibodies and EV concentration, or MFI of ROR1 and

252 HLA-I (R range 0.253-0.465, $P<0.05$; Table S6) in patients with AMR.

253 Moreover, a significant correlation was found between lymphocyte counts and EV concentration. The

254 number of lymphocytes and/or monocytes were also correlated to expression levels of HLA-II, CD25,

255 HLA-I, SSEA-4, and CD41b in AMR and R0 patients, and to the expression of CD2, SSEA-4, and

256 CD41b in ACR and R0 patients (Table S7). No significant correlations were observed between EV-

257 surface markers and age at heart transplant, or time to rejection onset.

258 A sub-analysis aiming to assess the sex-specific expression of EV surface antigens demonstrated a

259 selective over-expression of CD3, CD19, CD2, CD25, and CD20 in rejecting females, whereas CD41b

260 was over-expressed in male rejecting patients. In addition, the increase in EV concentration assessed by

261 CD9/CD63/CD81 MFI was more relevant in female patients with rejection, as compared to males (Table

262 S8).   Finally, we performed a correlation analysis between EMB findings and the expression of EV

11

263   markers. CD3, ROR1, SSEA-4, HLA-I, and CD41b MFI were directly correlated to the presence of

264   inflammatory infiltrate, myocytolisis, myocyte necrosis, and/or vasculitis in ACR patients (R range

265   0.239-0.513, $P<0.05$). HLA-II, SSEA-4, and HLA-I were correlated to the presence of inflammatory

266   infiltrate and vasculitis in AMR patients (R range 0.238-0.462, $P<0.05$; Table S9).

267   *Protein interactor network analysis*

268   Since secreted EV have been shown to mediate autocrine, paracrine and endocrine signaling, we

269   performed a theoretical analysis to predict possible protein-protein interactors. The network analysis

270   allowed identification of potential protein targets, biological pathways and molecular functions that could

271   be affected by EV-surface markers that were differentially expressed in rejecting vs. not rejecting

272   patients. "Hubs" and "bottlenecks" refer to proteins with greater numbers of protein connections or to

273   those occupying critical network positions, suggesting pivotal roles for the management of information

274   flow over the network (33) (Figure S1);. Except for HLA-E, hubs and bottlenecks in the interactor

275   networks for ACR and AMR were different: ABI1, CD247, ERBB3, JUN, and B2M were identified as

276   main interactors in ACR, whereas CD74, VAPA, SSR4, COPB1, PTCH1, DYNLL1, SGTA, RANBP9,

277   and ITGA6 were main interactors in AMR (Tables S10, and S11). The higher number of EV-marker

278   interactors in both ACR and AMR networks led to the enrichment of specific pathways related to the

279   immune system and signal transduction, involving the inflammatory response, intercellular

280   communication, cell survival, and apoptosis.

281

282   **DISCUSSION**

283   The present study highlights the diagnostic potential of circulating EV as biomarkers for monitoring

284   cardiac allograft rejection. We found that the total amount of circulating vesicles assessed by the

285   expression of specific surface antigens CD63, CD81, and CD9, discriminated between patients with and

286   without rejection. Both ACR and AMR patients showed an increase in EV concentration, compared to

12

R0. Nanoparticle tracking analysis (NTA), which strongly correlated with the expression of tetraspanins (CD63, CD9 and CD81), showed an increase in EV concentration for rejecting patients, specifically for small-sized EVs ($\leq$150 nm, the size specifically associated with exosomes). These results are consistent with the notion that the inflammatory state induces the release of microvesicles (34). Most importantly, plasma-derived EV carry a specific set of surface antigens, reflecting the change in immunologic profile of heart transplant recipients. The level of expression of specific, membrane-associated markers significantly diverged in patients with no rejection from those with rejection, and above all, different types of rejection were discriminated by EV profiling. Eleven of 37 analyzed surface antigens were differentially expressed in patients with ACR and AMR compared to patients without rejection. Six markers identified a cluster of patients with ACR, whereas nine markers identified patients with AMR. Finally, ROC curves revealed high performances for the evaluated EV markers, with 100% sensitivity reached for several markers (HLA-I, CD2 and SSEA-4 for ACR; ROR1, SSEA-4, HLA-II and CD41b for AMR). The diagnostic potential was further improved by combining MFI values of the 11 EV surface antigens differentially expressed between groups through a machine learning approach.

The accuracy of our computational approach resulted in a theoretical validation of ~89% and it stands at ~87% when the validation was performed on a separate cohort of patients, with a negligible overfitting effect of about 2%.

In light of what stated above, the immuno-profiling of plasma-derived EV and the integration of complex computational approaches in the management of patients after heart transplant, would help clinicians to discriminate between patients requiring EMB from those who may not require this procedure.

The major strength of EV profiling approach is that it resulted in a consistent (it has been validated on patients) and reliable (with a relevant diagnostic performance) non-invasive diagnostic test, that can eventually reduce the number of biopsies for non-rejecting patients. By using the proposed model to simulate the management of subjects included in the validation cohort (37 consecutively enrolled

311   patients), introducing blood sampling and EV analysis before the EMB procedure, we could have reduced

312   the number of patients selected for biopsy by 56.8% (flowchart in Figure 6). Unfortunately, three

313   rejecting patients would have missed the possibility to be correctly managed through EMB.

314   Another strength that should be considered in envisioning the profiling of EV as potential diagnostic

315   tool lies in the fact that by analyzing systemic circulating particles, clinicians can quickly grasp a more

316   complete picture of patient's status. Indeed, differentially expressed markers on the surface of EV in

317   blood may be more representative as compared to markers detected in tissue sample, which can be

318   distorted by necrosis and fibrotic areas. Although, we did not select cardiac specific EV, as to date there

319   is no specific antibody recognizing tissue specific vesicles, EV in blood presumably includes particles

320   released from injured areas of tissue, but preferentially exclude necrotic areas in which circulation has

321   ceased.

322   Other studies have evaluated profiling of circulating EV to non-invasively monitor cardiac allografts for

323   rejection. Kennel et al. performed proteomic analysis by liquid chromatography-tandem mass

324   spectrometry on serum-derived exosomes (small EV) collected from heart transplant recipients with no

325   rejection, ACR, and AMR(35). They found that allograft rejection alters the protein content of circulating

326   exosomes, giving them unique protein expression patterns, which are suitable as predictive and

327   prognostic biomarkers. Although very interesting, the approach used by Kennel at al. was based on

328   relatively complex methodologies and instrumentation. Here we propose the profiling of the surface of

329   EV which does not require lysis or digestion steps and can be performed using conventional flow

330   cytometers. Habertheuer et al. have recently shown that transplanted hearts release donor-specific

331   exosomes. In a murine model of heterotopic heart transplant, they elegantly showed that the cardiac

332   allograft releases a distinct pool of donor MHC-specific exosomes into recipient circulation. The signal

333   peaked during early stages of acute rejection with high accuracy(36) enabling the development of a very

334   specific and sensitive biomarker platform for allograft monitoring (36, 37). Compared to this study that

335 was carried out in a model of major histocompatibility mismatch using immunodeficient recipient mice,

336 our platform has been analyzed in a clinical setting, including immunocompetent recipients on

337 maintenance immuno-suppression, and provides comparable accuracy.

338 Quantitative changes in microRNA cargo of serum exosomes from heart transplant recipients has also

339 been demonstrated. Dewi and colleagues showed that microRNA miR-142-3p increased in case of

340 ACR(38). miR-142-3p is enclosed into secreted exosomes from T cells and targets specific messenger

341 RNA in endothelial cells, thus implying a role for T cell-derived EV in mediating graft rejection[38]. In

342 line with this hypothesis, we found that CD3 and CD2, T cell co-receptors, were both upregulated on the

343 surface of EV in patients with a diagnosis of ACR. It might be interesting, in the future, to assess whether

344 the EV expressing these surface co-receptors also carry miR-142-3p. This scenario would reinforce the

345 role of the endothelial-T cells axis in cell-mediated rejection.

346 EV surface antigens may also reflect activation of B-cells. The receptor tyrosine kinase ROR1, which is

347 a transmembrane protein highly expressed on the surface of leukemia cells, but not on normal B-

348 cells(39)·(40), was significantly overexpressed in both AMR and ACR patients as compared to controls.

349 However, none of the patients with rejection displayed proliferative hematologic disorders, thus ROR1

350 expression on EV might reflect an activation state of B-cells, which is not associated with a malignant

351 phenotype. Given the correlation with clinical, biochemical, and EMB parameters we found significantly

352 correlated between EV-surface markers and the numbers of circulating lymphocytes and monocytes in

353 rejecting patients. The total number of WBCs was not increased in patients with a diagnosis of rejection,

354 suggesting that EV number and profile may reflect the activation state of these cells and the systemic

355 inflammatory response in transplant rejection(41). EV surface markers were also correlated with the

356 presence of inflammatory infiltrate, myocytolisis, myocyte necrosis, and vasculitis on EMB, being

357 associated not only to the diagnosis of ACR/AMR, but also to the severity of the inflammatory response

358 triggered by rejection.

359 Although beyond the scope of the present paper, we hypothesized that EV antigens may exert active

360 biological functions providing autocrine and paracrine signals to target cells (19, 42)·(43). In this regard,

361 we performed a theoretical interactor network analysis which suggested that the large majority of proteins

362 up-regulated on EV of rejecting patients may have a potential role as ligand–receptor interactors for

363 several intercellular pathways involved in the inflammatory response to graft rejection. For instance,

364 circulating EV can act as extracellular stimuli for Jun (hub/bottleneck in ACR network), which controls

365 a number of cellular processes including differentiation, proliferation, and apoptosis through the

366 formation of heterodimer AP-1(44). This carries importance when considering that allograft treatment

367 with decoy oligodeoxynucleotides (ODN) targeting the transcription factor AP-1 delays acute rejection

368 and prolongs cardiac allograft survival in a rat transplant model(45). Interestingly, the network analysis

369 highlighted a possible EV-mediated induction of genes related to natural killer (NK) cells and these

370 findings are in line with recent tissue-based gene profiling unveiling the association of NK transcripts

371 with chronic allograft vasculopathy in AMR (46).

372 After stratification for sex, we found several EV markers selectively enriched in female rejecting patients.

373 In particular, the overexpression of surface antigens CD19 and CD 20 (both markers of B-cells) is

374 noteworthy, as it is known that estrogens amplify immuno-responses in women (47, 48). They act by

375 increasing total number of progenitor B cells (49), and inducing B cell activation (50).

376 The main limit of the present study is that the patients used for training and validation of the model did

377 not allow us for longitudinal-based cohort study, thus limiting the evaluation of our model as predictive

378 approach. Indeed, a longitudinal cohort would have allowed the demonstration of whether this approach

379 may identify rejection before the diagnosis made by EMB, and whether changes in EV related parameters

380 may even anticipate the histologic evidence of rejection, thus enabling the institution of an earlier and

381 perhaps less intrusive treatment. A second important issue is the absence of specific, cardiac-derived

382 antigens among the EV markers included in the analysis, thus excluding the possibility of grading the

383   vascular damage and cardiac damage related to rejection. Another potential limitation is the relatively

384   small sample size. Our selection strategy at training was based on a well-defined histological pattern at

385   EMB (see methods). This allowed us to evaluate highly selected patients and train the diagnostic model

386   on subjects that truly underwent rejection. On the other hand, this can be a limitation as the training of

387   the model does not include subjects with mild forms of rejection. However, the validation of the model

388   was performed on an unselected cohort of patients, thus suggesting a potential clinical application, even

389   if the present findings still have to be confirmed in larger prospective cohorts. Finally, we showed that

390   different types of rejection are associated with different EV phenotypes, but we cannot define whether

391   these phenotypes are specific for rejection, as the large majority of antigens might be theoretical

392   associated with other acute and chronic inflammatory diseases.

393   In conclusion, given its low cost, speed, and simplicity, as well as its high accuracy, the method here

394   described provides a connection between allograft phenotypes, biochemical indexes, and histology

395   parameters for the detection of different types of heart allograft rejection. Circulating plasma-derived EV

396   are a highly promising tool for characterising and monitoring cardiac allograft rejection. It does not

397   standalone as diagnostic biomarker that could completely replace EMB. The quantitative flow cytometer

398   analysis and the computational approach proposed here can act in synergy with tissue histology and offer

399   a tool to clinician for reducing the number of biopsies and selecting patients with the highest risk of

400   rejection for a closer follow-up.

416 **REFERENCES**

417 1. Yusen RD, Edwards LB, Dipchand AI, et al.: The Registry of the International Society for Heart and

418   Lung Transplantation: Thirty-third Adult Lung and Heart-Lung Transplant Report-2016; Focus

419   Theme: Primary Diagnostic Indications for Transplant. J Heart Lung Transplant 2016;35:1170-84.

420 2. Weber BN, Kobashigawa JA, Givertz MM: Evolving Areas in Heart Transplantation. JACC Heart

421   Fail 2017;5:869-78.

422 3. Lund LH, Edwards LB, Kucheryavaya AY, et al.: The registry of the International Society for Heart

423   and Lung Transplantation: thirty-first official adult heart transplant report--2014; focus theme:

424   retransplantation. J Heart Lung Transplant 2014;33:996-1008.

425 4. Stewart S, Winters GL, Fishbein MC, et al.: Revision of the 1990 working formulation for the

426   standardization of nomenclature in the diagnosis of heart rejection. J Heart Lung Transplant

427   2005;24:1710-20.

428 5. Berry GJ, Burke MM, Andersen C, et al.: The 2013 International Society for Heart and Lung

429   Transplantation Working Formulation for the standardization of nomenclature in the pathologic

430   diagnosis of antibody-mediated rejection in heart transplantation. J Heart Lung Transplant

431   2013;32:1147-62.

432 6. Hershberger RE, Starling RC, Eisen HJ, et al.: Daclizumab to prevent rejection after cardiac

433   transplantation. N Engl J Med 2005;352:2705-13.

434 7. Grimm M, Rinaldi M, Yonan NA, et al.: Superior prevention of acute rejection by tacrolimus vs.

435   cyclosporine in heart transplant recipients--a large European trial. Am J Transplant 2006;6:1387-97.

436 8. Wong RC, Abrahams Z, Hanna M, et al.: Tricuspid regurgitation after cardiac transplantation: an

437   old problem revisited. J Heart Lung Transplant 2008;27:247-52.

438 9. Nguyen V, Cantarovich M, Cecere R, Giannetti N: Tricuspid regurgitation after cardiac

439   transplantation: how many biopsies are too many? J Heart Lung Transplant 2005;24:S227-31.

440   10. Bishawi M, Zanotti G, Shaw L, et al.: Tricuspid Valve Regurgitation Immediately After Heart

441   Transplant and Long-Term Outcomes. Ann Thorac Surg 2019;107:1348-55.

442   11. Hamour IM, Burke MM, Bell AD, Panicker MG, Banerjee R, Banner NR: Limited utility of

443   endomyocardial biopsy in the first year after heart transplantation. Transplantation 2008;85:969-74.

444   12. Di Francesco A, Fedrigo M, Santovito D, et al.: MicroRNA signatures in cardiac biopsies and

445   detection of allograft rejection. J Heart Lung Transplant 2018;37:1329-40.

446   13. Duong Van Huyen JP, Tible M, Gay A, et al.: MicroRNAs as non-invasive biomarkers of heart

447   transplant rejection. Eur Heart J 2014;35:3194-202.

448   14. Halloran PF, Potena L, Van Huyen JD, et al.: Building a tissue-based molecular diagnostic system

449   in heart transplant rejection: The heart Molecular Microscope Diagnostic (MMDx) System. J Heart

450   Lung Transplant 2017;36:1192-200.

451   15. De Vlaminck I, Valantine HA, Snyder TM, et al.: Circulating cell-free DNA enables noninvasive

452   diagnosis of heart transplant rejection. Sci Transl Med 2014;6:241ra77.

453   16. Beck J, Oellerich M, Schulz U, et al.: Donor-Derived Cell-Free DNA Is a Novel Universal

454   Biomarker for Allograft Rejection in Solid Organ Transplantation. Transplant Proc 2015;47:2400-

455   3.

456   17. Maas SLN, Breakefield XO, Weaver AM: Extracellular Vesicles: Unique Intercellular Delivery

457   Vehicles. Trends Cell Biol 2017;27:172-88.

458   18. S ELA, Mager I, Breakefield XO, Wood MJ: Extracellular vesicles: biology and emerging

459   therapeutic opportunities. Nat Rev Drug Discov 2013;12:347-57.

460   19. Cervio E, Barile L, Moccetti T, Vassalli G: Exosomes for Intramyocardial Intercellular

461   Communication. Stem Cells Int 2015;2015:482171.

462   20. Pant S, Hilton H, Burczynski ME: The multifaceted exosome: biogenesis, role in normal and

463   aberrant cellular function, and frontiers for pharmacological and biomarker opportunities. Biochem

464   Pharmacol 2012;83:1484-94.

465   21. Revenfeld AL, Baek R, Nielsen MH, Stensballe A, Varming K, Jorgensen M: Diagnostic and

466   prognostic potential of extracellular vesicles in peripheral blood. Clin Ther 2014;36:830-46.

467   22. Barile L, Vassalli G: Exosomes: Therapy delivery tools and biomarkers of diseases. Pharmacology

468   & therapeutics 2017;174:63-78.

469   23. Boulanger CM, Loyer X, Rautou PE, Amabile N: Extracellular vesicles in coronary artery disease.

470   Nat Rev Cardiol 2017;14:259-72.

471   24. Haller PM, Stojkovic S, Piackova E, et al.: The association of P2Y12 inhibitors with pro-coagulatory

472   extracellular vesicles and microRNAs in stable coronary artery disease. Platelets 2019:1-8.

473   25. Sarkar A, Mitra S, Mehta S, Raices R, Wewers MD: Monocyte derived microvesicles deliver a cell

474   death message via encapsulated caspase-1. PLoS One 2009;4:e7140.

475   26. Wiklander OPB, Bostancioglu RB, Welsh JA, et al.: Systematic Methodological Evaluation of a

476   Multiplex Bead-Based Flow Cytometry Assay for Detection of Extracellular Vesicle Surface

477   Signatures. Front Immunol 2018;9:1326.

478   27. El Andaloussi S, Lakhal S, Mager I, Wood MJ: Exosomes for targeted siRNA delivery across

479   biological barriers. Adv Drug Deliv Rev 2013;65:391-7.

480   28. Koliha N, Wiencek Y, Heider U, et al.: A novel multiplex bead-based platform highlights the

481   diversity of extracellular vesicles. J Extracell Vesicles 2016;5:29975.

482   29. Andriolo G, Provasi E, Lo Cicero V, et al.: Exosomes From Human Cardiac Progenitor Cells for

483   Therapeutic Applications: Development of a GMP-Grade Manufacturing Method. Frontiers in

484   Physiology 2018;9.

485 30. Burrello J, Burrello A, Stowasser M, et al.: The Primary Aldosteronism Surgical Outcome Score for

486   the Prediction of Clinical Outcomes After Adrenalectomy for Unilateral Primary Aldosteronism.

487   Ann Surg 2019.

488 31. Meyer LS, Wang X, Susnik E, et al.: Immunohistopathology and Steroid Profiles Associated With

489   Biochemical Outcomes After Adrenalectomy for Unilateral Primary Aldosteronism. Hypertension

490   2018;72:650-7.

491 32. Scardoni G, Tosadori G, Pratap S, Spoto F, Laudanna C: Finding the shortest path with PesCa: a

492   tool for network reconstruction. F1000Res 2015;4:484.

493 33. Vella D, Zoppis I, Mauri G, Mauri P, Di Silvestre D: From protein-protein interactions to protein

494   co-expression networks: a new perspective to evaluate large-scale proteomic data. EURASIP J

495   Bioinform Syst Biol 2017;2017:6.

496 34. Puddu P, Puddu GM, Cravero E, Muscari S, Muscari A: The involvement of circulating

497   microparticles in inflammation, coagulation and cardiovascular diseases. Can J Cardiol

498   2010;26:140-5.

499 35. Kennel PJ, Saha A, Maldonado DA, et al.: Serum exosomal protein profiling for the non-invasive

500   detection of cardiac allograft rejection. J Heart Lung Transplant 2018;37:409-17.

501 36. Habertheuer A, Korutla L, Rostami S, et al.: Donor tissue-specific exosome profiling enables

502   noninvasive monitoring of acute rejection in mouse allogeneic heart transplantation. J Thorac

503   Cardiovasc Surg 2018;155:2479-89.

504 37. Vallabhajosyula P, Korutla L, Habertheuer A, et al.: Tissue-specific exosome biomarkers for

505   noninvasively monitoring immunologic rejection of transplanted tissue. J Clin Invest

506   2017;127:1375-91.

507 38. Sukma Dewi I, Celik S, Karlsson A, et al.: Exosomal miR-142-3p is increased during cardiac

508   allograft rejection and augments vascular permeability through down-regulation of endothelial

509   RAB11FIP2 expression. Cardiovasc Res 2017;113:440-52.

510 39. Choi MY, Widhopf GF, 2nd, Wu CC, et al.: Pre-clinical Specificity and Safety of UC-961, a First-

511   In-Class Monoclonal Antibody Targeting ROR1. Clin Lymphoma Myeloma Leuk 2015;15

512   Suppl:S167-9.

513 40. Saleh RR, Antras JF, Peinado P, et al.: Prognostic value of receptor tyrosine kinase-like orphan

514   receptor (ROR) family in cancer: A meta-analysis. Cancer Treat Rev 2019;77:11-9.

515 41. Burrello J, Monticone S, Gai C, Gomez Y, Kholia S, Camussi G: Stem Cell-Derived Extracellular

516   Vesicles and Immune-Modulation. Front Cell Dev Biol 2016;4:83.

517 42. Margolis L, Sadovsky Y: The biology of extracellular vesicles: The known unknowns. PLoS Biol

518   2019;17:e3000363.

519 43. Segura E, Amigorena S, Thery C: Mature dendritic cells secrete exosomes with strong ability to

520   induce antigen-specific effector immune responses. Blood Cells Mol Dis 2005;35:89-93.

521 44. Ameyar M, Wisniewska M, Weitzman JB: A role for AP-1 in apoptosis: the case for and against.

522   Biochimie 2003;85:747-52.

523 45. Holschermann H, Stadlbauer TH, Wagner AH, et al.: STAT-1 and AP-1 decoy oligonucleotide

524   therapy delays acute rejection and prolongs cardiac allograft survival. Cardiovasc Res 2006;71:527-

525   36.

526 46. Loupy A, Duong Van Huyen JP, Hidalgo L, et al.: Gene Expression Profiling for the Identification

527   and Classification of Antibody-Mediated Heart Rejection. Circulation 2017;135:917-35.

528 47. Khan D, Ansar Ahmed S: The Immune System Is a Natural Target for Estrogen Action: Opposing

529   Effects of Estrogen in Two Prototypical Autoimmune Diseases. Front Immunol 2015;6:635.

530 48. Morgan AE, Dewey E, Mudd JO, et al.: The role of estrogen, immune function and aging in heart

531   transplant outcomes. Am J Surg 2019;218:737-43.

532 49. Bouman A, Heineman MJ, Faas MM: Sex hormones and the immune response in humans. Hum

533   Reprod Update 2005;11:411-23.

534 50. Ansar Ahmed S, Penhale WJ, Talal N: Sex hormones, immune responses, and autoimmune diseases.

535   Mechanisms of sex hormone action. Am J Pathol 1985;121:531-51.

536

TABLE LEGENDS

Table 1 –**Characteristics of patients from the training cohort.** Sex, age at heart transplant (HT), endomyocardial biopsy (EMB) characteristics, cellular rejection score (RS) and HLA-I/II donor- specific and nonspecific antibodies (DSA) in patients from the training cohort, without rejection (R0; n=33), with cellular-mediated (ACR; n=11) or with antibody-mediated rejection (AMR; n=9). *P*-values of less than 0.05 were considered significant (in bold).

FIGURE LEGENDS

Figure 1 – **EV characterization.** Characterization of circulating extracellular vesicles (EV) from patients of the training cohort with cellular-mediated rejection (ACR; orange; n=11), antibody-mediated rejection (AMR blue; n=9), compared to controls without graft rejection (rejection 0, R0; green; n=33). (A) Patient samples underwent serial centrifugation and then EV were characterized by nanoparticle tracking analysis (NTA) and standardized multiplex flow cytometry for the evaluation of 37 different EV surface antigens. (B) Western blot analysis of plasma and EV isolated by bead immuno-capture (n=4) for 2 EV markers (TSG101 and CD81) and a potential contaminant (Apolipoprotein, B48). (C) Median fluorescence intensity (MFI, %) of CD9, CD63, and CD81 by flow cytometric analysis. (D) Cumulative distribution plot combining EV concentration (n/mL; y axis) and diameter (nm; x axis). (E) Correlation between EV concentration and CD9-CD63-CD81 MFI. The regression line is depicted in red, with a 95% confidence interval. Data are expressed as median and interquartile range (panel C). *P* values < 0.05 were considered significant (*$P < 0.05$; **$P < 0.01$).

Figure 2 – **EV-surface markers.** Median fluorescence intensity (MFI, expressed as a percentage [%], after normalization with mean MFI of CD9, CD63, and CD81) for differentially expressed EV surface markers in patients with cellular-mediated rejection (ACR; orange; n=11), antibody-mediated rejection

561 (AMR; blue; n=9), or without graft rejection (rejection 0, R0; green; n=33). (A) EV surface markers were

562 divided into three groups in which EV markers were significantly increased: in patients with ACR *vs.* R0

563 (left), in patients with AMR *vs.* R0 (right), and both rejection groups *vs.* R0 (middle). Patients with ACR

564 are represented in orange (n=11), AMR in blue (n=9), and the R0 group in green (n=33). Horizontal lines

565 on the circles indicate significant increases compared to R0 ($P < 0.05$). (B) Heat map representing EV

566 surface marker expression in patients stratified for diagnosis (red, low fluorescence; green, high

567 fluorescence)..

568

569 *Figure 3* – **Diagnostic performances of EV surface markers.** Diagnostic performances of EV surface

570 markers differentially expressed in patients without rejection (R0) compared to cellular-mediated

571 rejection (ACR; n=44; panels A and C) and antibody-mediated rejection (AMR; n=42; panels B and D).

572 The area under the curve (AUC), asymptotic difference compared to the referral line (dashed grey line),

573 sensitivity, and specificity are reported for each marker.

574

575 *Figure 4* – **Diagnostic Modelling.** Random forest (RF) model for the diagnosis of allograft rejection

576 using MFI values for the 11 EV surface markers differentially expressed among patients with cellular-

577 mediated rejection (ACR; orange; n=11), antibody-mediated rejection (AMR blue; n=9), compared to

578 controls without graft rejection (rejection 0, R0; green; n=33). (A) Double level RF model. Level 1

579 identifies patients with graft rejection, whereas Level 2 distinguishes between AMR and ACR. (B)

580 Combined model discriminating between R0, ACR, and AMR in a single step. Representative

581 classification trees and confusion matrix at training and internal validation of the model are reported for

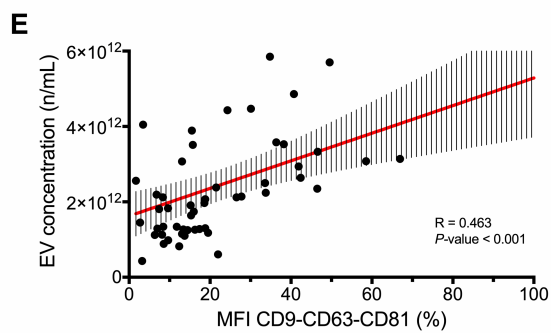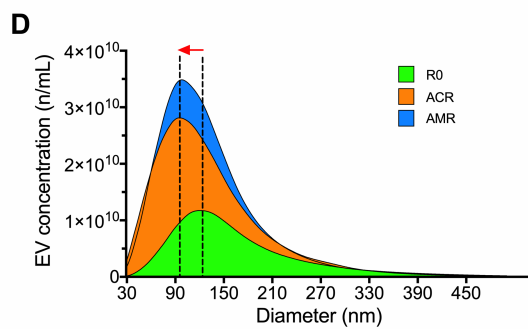582 each model. The sole missing patient with rejection is highlighted in red.
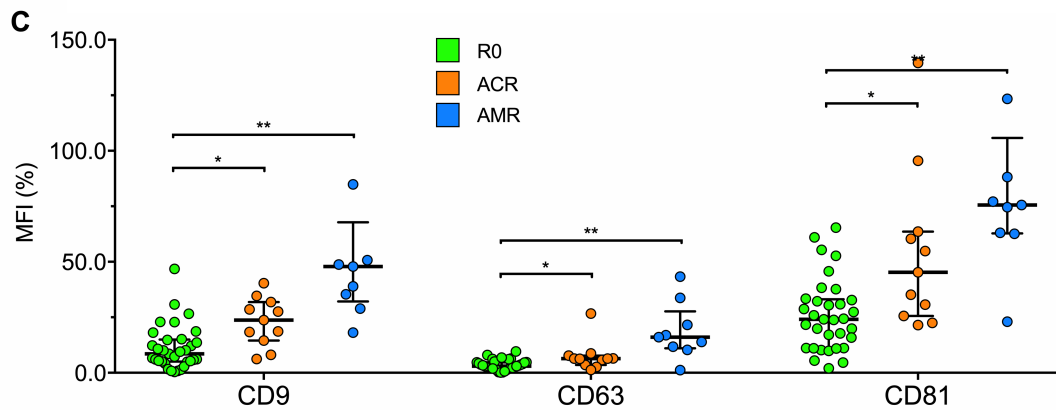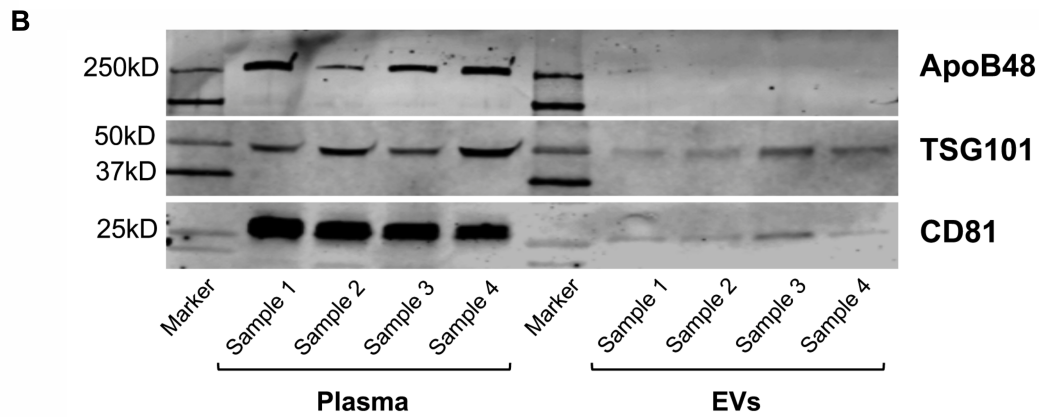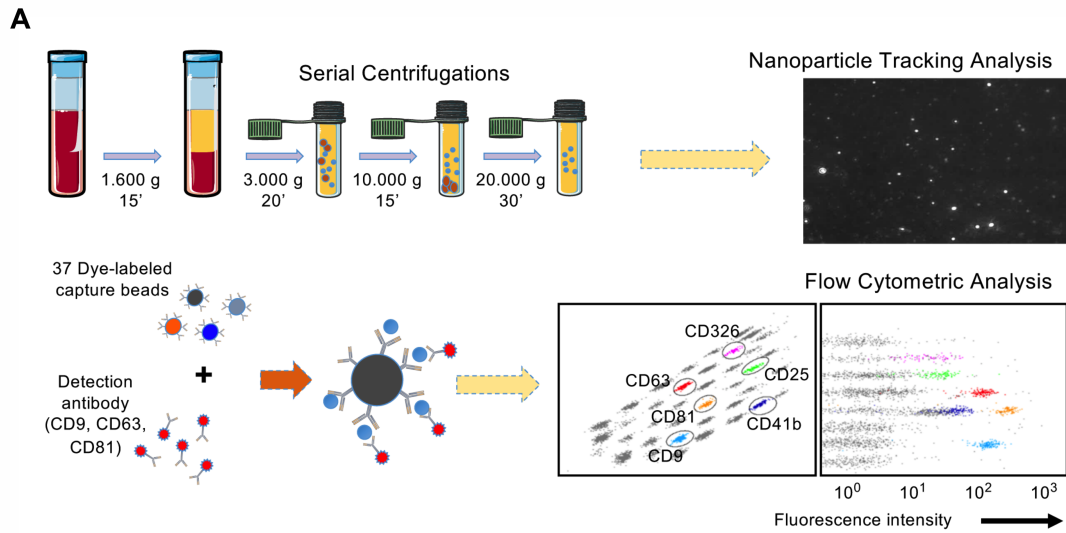
583

584 *Figure 5 –* **External validation of random forest diagnostic models**. The random forest models (level

585 1, level 2, and the combined model) were validated on an independent external cohort (n=37). (A) Heat

586 map representing EV surface marker expression in patients from the external validation cohort (n=37):

587 acute cellular rejection (ACR; orange; n=13), antibody-mediated rejection (AMR; blue; n=4), or without

588 graft rejection (rejection 0, R0; green; n=20). (B, C, and D) Confusion matrix reporting accuracy, real,

589 and predicted diagnosis, are reported for each model. Missed rejecting patients are underlined in red.
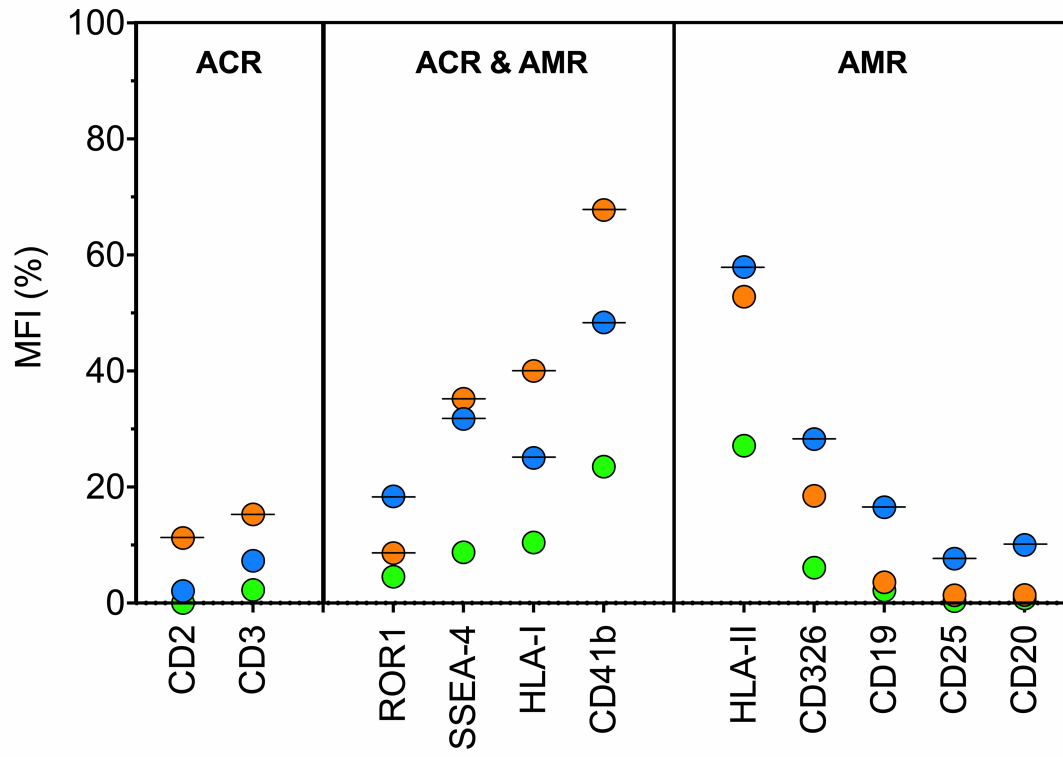
590

591 *Figure 6 –* **Simulated application of EV profiling in clinical practice.** The random forest model (level

592 1) was applied to the validation cohort (n=37) to select patients for endomyocardial biopsy (EMB)

593 (A) Management of heart transplanted patients using EMB as gold standard; all patients are correctly

594 managed (accuracy 100%; number of EMB = 37). (B) Flow chart integrating EV profiling in patient

595 management; 34 of 37 patients would be correctly managed (accuracy 91.9%; number of EMB = 16 [-

596 56.8%]); 3 patients (in red) were misclassified and would miss the possibility to performed EMB.

597

598

A

Serial Centrifugations

Nanoparticle Tracking Analysis

1.600 g 15' → 3.000 g 20' → 10.000 g 15' → 20.000 g 30'

37 Dye-labeled capture beads

Detection antibody (CD9, CD63, CD81)

Flow Cytometric Analysis

CD326
CD63
CD25
CD81
CD41b
CD9

Fluorescence intensity

10^0 10^1 10^2 10^3

B

250kD — ApoB48

50kD
37kD — TSG101

25kD — CD81

Marker Sample 1 Sample 2 Sample 3 Sample 4 | Marker Sample 1 Sample 2 Sample 3 Sample 4

Plasma | **EVs**

C

MFI (%)

R0
ACR
AMR

CD9 CD63 CD81

D

EV concentration (n/mL)

R0
ACR
AMR

Diameter (nm)

E

EV concentration (n/mL)

MFI CD9-CD63-CD81 (%)

R = 0.463
P-value < 0.001

599

A

B

600

A

R0 *vs.* ACR [n=44]	AUC (95% CI)	*P*-value	Sensitivity (%)	Specificity (%)
CD3	0.848 (0.736-0.961)	**0.001**	90.9	75.8
CD2	0.829 (0.704-0.955)	**0.001**	100.0	81.8
ROR1	0.771 (0.627-0.915)	**0.008**	90.9	66.7
SSEA-4	0.832 (0.711-0.952)	**0.001**	100.0	63.6
HLA-I	0.939 (0.869-1.000)	**0.000**	100.0	87.9
CD41b	0.815 (0.653-0.978)	**0.002**	90.9	60.6

B

R0 *vs.* AMR [n=42]	AUC (95% CI)	*P*-value	Sensitivity (%)	Specificity (%)
CD19	0.795 (0.648-0.942)	**0.007**	88.9	78.8
HLA-II	0.788 (0.653-0.922)	**0.009**	100.0	69.7
CD25	0.727 (0.568-0.886)	**0.039**	88.9	75.8
ROR1	0.879 (0.776-0.981)	**0.001**	100.0	75.8
SSEA-4	0.820 (0.692-0.947)	**0.004**	100.0	60.6
HLA-I	0.872 (0.757-0.988)	**0.001**	88.9	75.8
CD41b	0.778 (0.619-0.937)	**0.011**	100.0	51.5
CD326	0.788 (0.597-0.979)	**0.009**	88.9	69.7
CD20	0.798 (0.651-0.945)	**0.007**	88.9	81.8

C

D

601
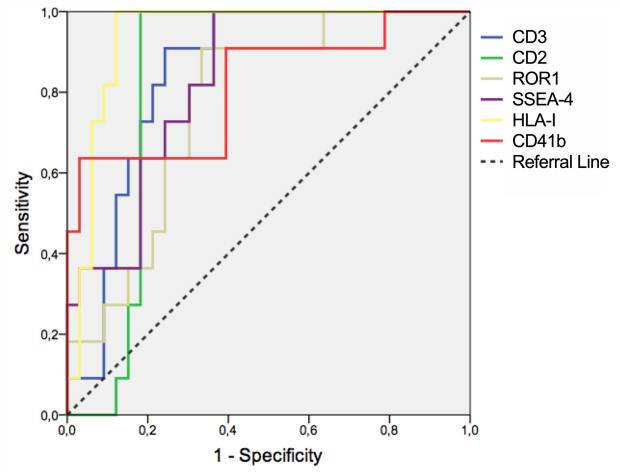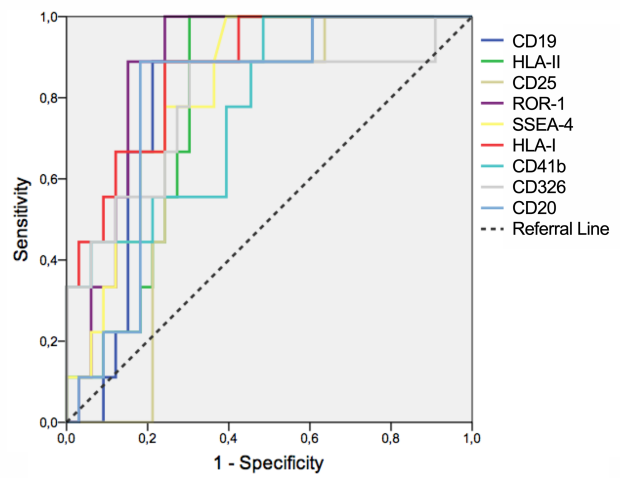
A
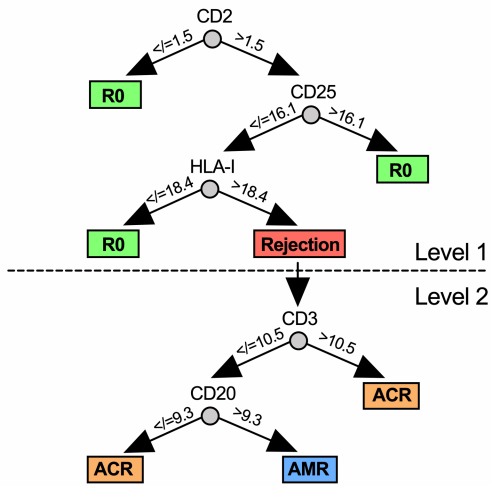
Level 1		DETECTED at TRAINING		INTERNAL VALIDATION	
		R0	Rejection	R0	Rejection
REAL	R0	**33**	0	**28**	5
	Rejection	0	**20**	1	**19**
Accuracy		100.0%		88.7%	

Level 2		DETECTED at TRAINING		INTERNAL VALIDATION	
		ACR	AMR	ACR	AMR
REAL	ACR	**11**	0	**10**	1
	AMR	1	**8**	2	**7**
Accuracy		95.0%		85.0%	

B

602
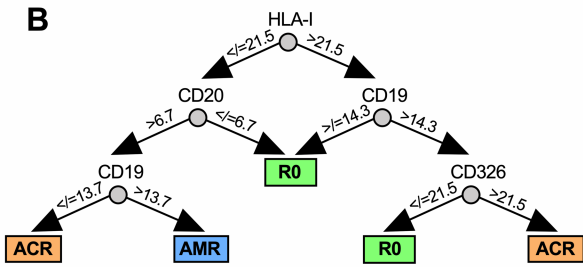
Combined		DETECTED at TRAINING			INTERNAL VALIDATION		
		R0	ACR	AMR	R0	ACR	AMR
REAL	R0	**33**	0	0	**27**	0	6
	ACR	0	**11**	0	0	**10**	1
	AMR	0	0	**9**	1	1	**7**
Accuracy		100.0%			83.0%		

A

													Level 1	Detected Level 2	Combined

B
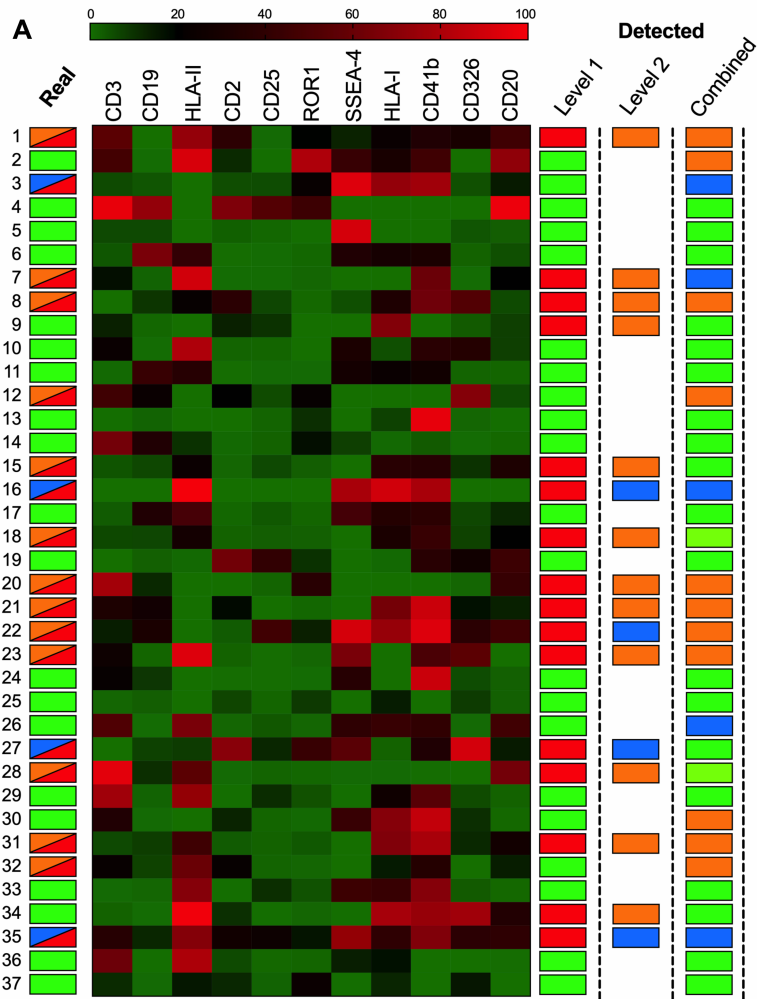
Level 1		DETECTED	
		R0	Rejection
REAL	R0	**18**	2
	Rejection	3	**14**
Accuracy		86.5%	

C

Level 2		DETECTED	
		ACR	AMR
REAL	ACR	**10**	1
	AMR	0 + 2 R0	**3**
Accuracy		81.3%	

D

Combined		DETECTED		
		R0	ACR	AMR
REAL	R0	**17**	2	1
	ACR	3	**9**	1
	AMR	1	0	**3**
Accuracy		78.4%		

603

604